

Cavity-assisted spontaneous emission as a single-photon source: Pulse shape and efficiency of one-photon Fock state preparation

M. Khanbekyan* and D.-G. Welsch

Theoretisch-Physikalisches Institut, Friedrich-Schiller-Universität Jena, Max-Wien-Platz 1, D-07743 Jena, Germany

C. Di Fidio and W. Vogel

Arbeitsgruppe Quantenoptik, Institut für Physik, Universität Rostock, D-18051 Rostock, Germany

(Dated: November 15, 2018)

Within the framework of exact quantum electrodynamics in dispersing and absorbing media, we have studied the quantum state of the radiation emitted from an initially in the upper state prepared two-level atom in a high- Q cavity, including the regime where the emitted photon belongs to a wave packet that simultaneously covers the areas inside and outside the cavity. For both continuing atom-field interaction and short-term atom-field interaction, we have determined the spatio-temporal shape of the excited outgoing wave packet and calculated the efficiency of the wave packet to carry a one-photon Fock state. Furthermore, we have made contact with quantum noise theories where the intracavity field and the field outside the cavity are regarded as approximately representing independent degrees of freedom such that two separate Hilbert spaces can be introduced.

PACS numbers: 42.50.Lc, 42.50.Dv, 03.50.De, 05.30.-d

I. INTRODUCTION

The interaction of a single atom with a quantized radiation-field mode in a high- Q cavity has played an important role not only due to its conceptual relevance, but also because it serves as a basic ingredient in various schemes in quantum optics and related fields such as quantum information science (for a review see, e.g., Refs. [1, 2]). In fact, cavity quantum electrodynamics (QED) has allowed the generation and processing of nonclassical radiation and offered novel radiation sources such as the single-atom maser [3, 4] and laser [5, 6, 7, 8] and the ion-trap laser [9, 10, 11, 12]. In this context, quantum control of single-photon emission from an atom in a cavity for generating single-photon Fock states on demand has been an essential prerequisite [13]. In particular, single-photon Fock state generation of high efficiency, as boosted by the well-pronounced line spectra of cavity fields, has been a key requirement in various applications such as quantum cryptography [14, 15] or quantum networking for distribution and processing of quantum information [16, 17]. Recently, single-photon sources operating on the basis of adiabatic passage with just one atom trapped in a high- Q optical cavity has been realized [18, 19, 20]. In this way, generation of single-photons of known circular polarization has been possible [21]. Moreover, adjustment of the spatio-temporal profile of single-photon pulses has been achieved [22, 23].

In view of the very wide-spread applications of cavity-assisted single-photon sources, it is of great importance to carefully study the quantum state of the field escaping from a cavity. Let us consider the simplest case of a two-level atom that near-resonantly interacts with a

narrow-band cavity-field mode. On a time scale that is sufficiently short compared to the inverse bandwidth of the mode, the radiative and non-radiative cavity losses may be disregarded, and the atom-field dynamics can be described by the familiar Jaynes-Cummings model [24]. Clearly, for longer times, the atom-cavity system cannot longer be regarded as being a closed system, and the losses must be taken into account. Since the wanted outgoing field represents, from the point of view of the atom-cavity system, radiative losses, the study of the input-output problem necessarily requires inclusion in the theory of the effects of losses.

There are primarily two approaches to the problem, namely the approach based on quantum noise theory and the one based on macroscopic QED. In quantum noise theory (QNT), the fields inside and outside a cavity are regarded as representing independent degrees of freedom, as it would be the case if the cavity were bounded by perfectly reflecting walls [25, 26, 27]. Accordingly, QNT is based on discrete and continuous mode expansions of the fields inside and outside the cavity, respectively, so that inside- and outside-field operators can be regarded as being commuting quantities. In order to *a posteriori* take into account the input-output coupling due to non-perfectly reflecting mirrors, each intracavity mode is linearly coupled to the continuum of the external modes, which is regarded as playing the role of a dissipative system. Its effect on the intracavity modes is treated in Markovian approximation, leading to quantum Langevin equations for the intracavity-mode operators, where the incoming external field gives rise to the operator Langevin forces therein. Additionally to the radiative losses associated with a normally wanted input-output coupling, there are always unwanted losses such as absorption and scattering losses. They can be straightforwardly included in the quantum Langevin equations by coupling the intracavity modes to additional dissipa-

*E-mail address: mkh@tpi.uni-jena.de

tive systems and treating these interactions in Markovian approximation [28]. Alternatively to the concept of quantum Langevin equations, dissipation can be described by using the concept of master equations (see, e.g. Refs [29, 30, 31]). There are different methods to solve master equations, for example, the method of quantum trajectories (see, e.g. Refs. [32, 33, 34]). In order to find the field escaping from the cavity, the quantum Langevin equations (or the equivalent master equations) are completed with input–output relations, which relate the output field to the input field and the intracavity field.

In macroscopic QED, the system is described on the basis of the respective macroscopic Maxwell equations [35, 36]. By starting from an ordinary continuous-mode expansion of the electromagnetic field in the presence of nonabsorbing linear media, it can be shown that in some approximation a description of the fields inside and outside a cavity in terms of quantum Langevin equations and input–output relations, respectively, as used in QNT can indeed be given [37, 38]. In another version of QED [39, 40], solutions of Maxwell’s equations are constructed by using Feshbach’s projection formalism [41]. By means of the appropriately chosen boundary conditions a decomposition of the field can be performed which renders it possible to catch up with the description of the cavity system within the framework of QNT. The method can be extended also to the case of overlapping cavity modes in the case of lower Q values. An alternative approach is based on an expansion of the fields inside and outside a cavity into nonorthogonal Fox-Li modes [42]. In this approach, however, the interaction energy between the cavity modes and the external modes vanishes and the input–output coupling arises from the non-zero commutator between the fields inside and outside the cavity.

Allowing for dispersing and absorbing media, one can also use macroscopic QED to include in the theory the effect of unwanted losses [43], which, in agreement with QNT, can be shown to become manifest in additional damping terms and the associated fluctuation forces in the quantum Langevin equations. In contrast, inclusion in the input–output relations of the effect of unwanted losses is not straightforward since it cannot be deduced from the interaction Hamiltonians used in QNT [43, 44, 45]. Particularly, input–output relations suggested by QNT do not describe the effect of unwanted losses on the output field which is induced by the reflected input field.

The input–output relations can be used to introduce a many-mode characteristic function of the quantum state of the output field, from which the quantum state can be inferred in terms of phase-space functions. In Ref. [43], explicit results are given for the case, when the time necessary to prepare an intracavity mode in some quantum state is sufficiently short compared to the decay time of this mode so that the preparation process may be disregarded and instead, an initial condition can be set for the quantum state of the intracavity mode [43]. Furthermore,

it is assumed that the fields inside and outside the cavity can be regarded as being effectively commuting quantities at equal times. In this way, the mode structure of the output field is determined, and the Wigner function of the quantum state of the relevant output mode—the one that is related to the excited intracavity-mode—is expressed in terms of the Wigner functions of the quantum states of the intracavity mode, the incoming field, and the radiationless dissipative system. Needless to say that the simplifying assumption of short preparation limits the scope of the results in general.

In the present paper we generalize the approach based on macroscopic QED in dispersing and absorbing media, with the aim to renounce the approximation that the electromagnetic fields inside and outside a cavity represent independent degrees of freedom. Instead, we treat the electromagnetic field as an entity. Further, we include in the theory the preparation process in order to go beyond the regime of short-time preparation. We work out the theory for the case where the quantum state of the outgoing field results from the resonant interaction of the electromagnetic field with a single two-level atom initially prepared in the upper state. Considering a source-quantity representation of the electromagnetic field and treating the atom–field interaction in rotating-wave approximation, we examine the mode structure of the outgoing field as well as the efficiency of the excited outgoing mode to carry a single-photon Fock state. We finally compare the results with the ones obtained within the framework of QNT.

The paper is organized as follows. The basic equations for the resonant interaction of a two-level atom with a cavity-assisted electromagnetic field are given in Sec. II. In Sec. III, the Wigner function of the quantum state of the excited outgoing wave packet and the shape of the wave packet are studied for different atom–field interaction times and a comparison with QNT is made. A summary and some concluding remarks are given in Sec. IV.

II. BASIC EQUATIONS

The starting point of QED are the macroscopic Maxwell equations for the medium-assisted electromagnetic field coupled to the equations of motion of the active atomic sources considered, where the effect of the medium is described by appropriately chosen constitutive equations. In particular, the effect of a locally responding, inhomogeneous, linear dielectric, which we will focus on throughout the paper, can be described by a spatially varying (relative) permittivity $\varepsilon(\mathbf{r}, \omega)$, which is a complex function of frequency,

$$\varepsilon(\mathbf{r}, \omega) = \varepsilon'(\mathbf{r}, \omega) + i\varepsilon''(\mathbf{r}, \omega), \quad (1)$$

with the real and imaginary parts $\varepsilon'(\mathbf{r}, \omega)$ and $\varepsilon''(\mathbf{r}, \omega)$, respectively, being related to each other via the Kramers–Kronig relations.

A. Quantization scheme

To be more specific, let us consider N atoms that interact with the electromagnetic field in the presence of a dielectric medium. Applying the multipolar-coupling scheme in electric dipole approximation, we may write the Hamiltonian that governs the temporal evolution of the overall system, which consists of the electromagnetic field, the dielectric medium (including the dissipative degrees of freedom), and the atoms coupled to the field, in the form [35, 36]

$$\hat{H} = \int d^3r \int_0^\infty d\omega \hbar\omega \hat{\mathbf{f}}^\dagger(\mathbf{r}, \omega) \cdot \hat{\mathbf{f}}(\mathbf{r}, \omega) + \sum_A \sum_k \hbar\omega_{Ak} \hat{S}_{Akk} - \sum_A \hat{\mathbf{d}}_A \cdot \hat{\mathbf{E}}(\mathbf{r}_A). \quad (2)$$

In this equation, the first term is the Hamiltonian of the field–medium system, where the bosonic fields $\hat{\mathbf{f}}(\mathbf{r}, \omega)$ and $\hat{\mathbf{f}}^\dagger(\mathbf{r}, \omega)$,

$$[\hat{f}_\mu(\mathbf{r}, \omega), \hat{f}_{\mu'}^\dagger(\mathbf{r}', \omega')] = \delta_{\mu\mu'} \delta(\omega - \omega') \delta^{(3)}(\mathbf{r} - \mathbf{r}'), \quad (3)$$

$$[\hat{f}_\mu(\mathbf{r}, \omega), \hat{f}_{\mu'}(\mathbf{r}', \omega')] = 0, \quad (4)$$

play the role of the canonically conjugate system variables. The second term is the Hamiltonian of the atoms, where the \hat{S}_{Akk} are the atomic flip operators for the A th atom,

$$\hat{S}_{Akk} = |k'\rangle_{AA}\langle k|, \quad (5)$$

with the $|k\rangle_A$ being the energy eigenstates of the A th atom. Finally, the last term is the atom–field coupling energy, where

$$\hat{\mathbf{d}}_A = \sum_{kk'} \mathbf{d}_{Akk'} \hat{S}_{Akk'} \quad (6)$$

is the electric dipole moment of the A th atom ($\mathbf{d}_{Akk'} = \langle k| \hat{\mathbf{d}}_A |k'\rangle_A$), and the medium-assisted electric field $\hat{\mathbf{E}}(\mathbf{r})$ can be expressed in terms of the variables $\hat{\mathbf{f}}(\mathbf{r}, \omega)$ and $\hat{\mathbf{f}}^\dagger(\mathbf{r}, \omega)$ as follows [49]:

$$\hat{\mathbf{E}}(\mathbf{r}) = \hat{\mathbf{E}}^{(+)}(\mathbf{r}) + \hat{\mathbf{E}}^{(-)}(\mathbf{r}), \quad (7)$$

$$\hat{\mathbf{E}}^{(+)}(\mathbf{r}) = \int_0^\infty d\omega \hat{\mathbf{E}}(\mathbf{r}, \omega), \quad \hat{\mathbf{E}}^{(-)}(\mathbf{r}) = [\hat{\mathbf{E}}^{(+)}(\mathbf{r})]^\dagger, \quad (8)$$

$$\hat{\mathbf{E}}(\mathbf{r}, \omega) = i\sqrt{\frac{\hbar}{\varepsilon_0\pi}} \frac{\omega^2}{c^2} \int d^3r' \sqrt{\varepsilon''(\mathbf{r}', \omega)} \mathbf{G}(\mathbf{r}, \mathbf{r}', \omega) \cdot \hat{\mathbf{f}}(\mathbf{r}', \omega), \quad (9)$$

where the classical (retarded) Green tensor $\mathbf{G}(\mathbf{r}, \mathbf{r}', \omega)$ is the solution to the equation

$$\nabla \times \nabla \times \mathbf{G}(\mathbf{r}, \mathbf{r}', \omega) - \frac{\omega^2}{c^2} \varepsilon(\mathbf{r}, \omega) \mathbf{G}(\mathbf{r}, \mathbf{r}', \omega) = \delta^{(3)}(\mathbf{r} - \mathbf{r}') \quad (10)$$

and satisfies the boundary condition at infinity, i.e., $\mathbf{G}(\mathbf{r}, \mathbf{r}', \omega) \rightarrow 0$ if $|\mathbf{r} - \mathbf{r}'| \rightarrow \infty$.

B. Two-level atom in a cavity

Let us focus on a single two-level atom at position z_A inside a high- Q cavity and use the model of Ley and Loudon [46], i.e., a one-dimensional cavity in z -direction which is bounded by a perfectly reflecting mirror at the left-hand side and a fractionally transparent mirror at the right-hand side, and a linearly polarized electromagnetic field which propagates along the z axis (Fig. 1). Regarding the cavity as a multi-layer dielectric system and restricting our attention to resonant atom–field interaction, we may start from the one-dimensional version of the Hamiltonian (2) and apply the rotating-wave approximation to the atom–field interaction, leading to

$$\hat{H} = \int dz \int_0^\infty d\omega \hbar\omega \hat{f}^\dagger(z, \omega) \hat{f}(z, \omega) + \hbar\omega_0 \hat{S}_{22} - \left[d_{21} \hat{S}_{12}^\dagger \hat{E}^{(+)}(z_A) + \text{H.c.} \right] \quad (11)$$

($\hat{S}_{k'k} \equiv \hat{S}_{Akk}$), where ω_0 is the atomic transition frequency.

In what follows we assume that the atom is initially (at time $t=0$) prepared in the upper state $|2\rangle$ and the rest of the system, i.e., the combined system that consists of the electromagnetic field and the cavity, is in the ground state $|\{0\}\rangle$. We may therefore expand the state vector of the overall system at a later time t ($t \geq 0$) as

$$|\psi(t)\rangle = C_2(t) e^{-i\omega_0 t} |2\rangle |\{0\}\rangle + \int dz \int_0^\infty d\omega C_1(z, \omega, t) e^{-i\omega t} |1\rangle \hat{f}^\dagger(z, \omega) |\{0\}\rangle, \quad (12)$$

where $|1\rangle$ is the lower atomic state, and $\hat{f}^\dagger(z, \omega) |\{0\}\rangle$ is a single-quantum excited state of the combined field–cavity system. It is not difficult to prove that the Schrödinger equation for $|\psi(t)\rangle$ then leads to the following system of differential equations for the probability amplitudes $C_2(t)$ and $C_1(z, \omega, t)$:

$$\dot{C}_2 = -\frac{d_{21}}{\sqrt{\pi\hbar\varepsilon_0\mathcal{A}}} \int_0^\infty d\omega \frac{\omega^2}{c^2} \int dz \sqrt{\varepsilon''(z, \omega)} \times G(z_A, z, \omega) C_1(z, \omega, t) e^{-i(\omega - \omega_0)t}, \quad (13)$$

$$\dot{C}_1(z, \omega, t) = \frac{d_{21}^*}{\sqrt{\pi\hbar\varepsilon_0\mathcal{A}}} \frac{\omega^2}{c^2} \sqrt{\varepsilon''(z, \omega)} \times G^*(z_A, z, \omega) C_2(t) e^{i(\omega - \omega_0)t} \quad (14)$$

(\mathcal{A} , mirror area). Substituting the formal solution of Eq. (14) [with the initial condition $C_1(z, \omega, 0) = 0$],

$$C_1(z, \omega, t) = \frac{d_{21}^*}{\sqrt{\pi\hbar\varepsilon_0\mathcal{A}}} \frac{\omega^2}{c^2} \sqrt{\varepsilon''(z, \omega)} G^*(z_A, z, \omega) \times \int_0^t dt' C_2(t') e^{i(\omega - \omega_0)t'}, \quad (15)$$

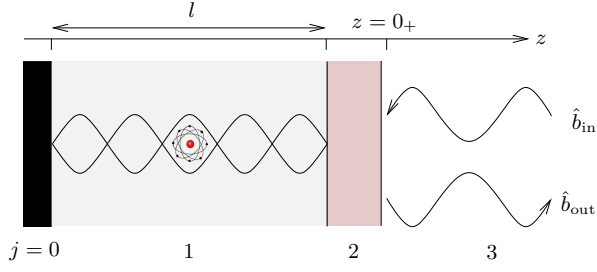


FIG. 1: Scheme of the system. The fractionally transparent mirror of the cavity (region 2) is modeled by a dielectric plate, and the atom inside the cavity (region 1) can be embedded in some dielectric medium.

into Eq. (13) and employing the integral relation

$$\text{Im} G(z_1, z_2, \omega) = \frac{\omega^2}{c^2} \int dz \varepsilon''(z, \omega) G(z_1, z, \omega) G^*(z_2, z, \omega), \quad (16)$$

we obtain the integro-differential equation

$$\dot{C}_2(t) = \int_0^t dt' K(t-t') C_2(t'), \quad (17)$$

where the integral kernel $K(t)$ reads

$$K(t) = -\frac{|d_{21}|^2}{\pi \hbar \epsilon_0 \mathcal{A}} \int_0^\infty d\omega \frac{\omega^2}{c^2} e^{-i(\omega - \omega_0)t} \text{Im} G(z_A, z_A, \omega). \quad (18)$$

We now recall that the spectral response of the cavity field is determined by the Green function $G(z, z', \omega)$ (see Appendix A). For a sufficiently high- Q cavity, the excitation spectrum effectively turns into a quasi-discrete set of lines of mid-frequencies ω_k and widths Γ_k , according to the poles of the Green function at the complex frequencies

$$\Omega_k = \omega_k - \frac{1}{2}i\Gamma_k, \quad (19)$$

where the line widths are much smaller than the line separations,

$$\Gamma_k \ll \frac{1}{2}(\omega_{k+1} - \omega_{k-1}). \quad (20)$$

In this case, we can divide the ω axis into intervals $\Delta_k = [\frac{1}{2}(\omega_{k-1} + \omega_k), \frac{1}{2}(\omega_k + \omega_{k+1})]$ and rewrite Eq. (18) as

$$K(t) = -\frac{|d_{21}|^2}{\pi \hbar \epsilon_0 \mathcal{A}} \sum_k \int_{\Delta_k} d\omega \frac{\omega^2}{c^2} e^{-i(\omega - \omega_0)t} \text{Im} G(z_A, z_A, \omega). \quad (21)$$

Inserting Eq. (21) into Eq. (17), we obtain

$$\dot{C}_2(t) = -\frac{|d_{21}|^2}{\pi \hbar \epsilon_0 \mathcal{A}} \sum_k \int_0^t dt' \int_{\Delta_k} d\omega \frac{\omega^2}{c^2} \times e^{-i(\omega - \omega_0)(t-t')} \text{Im} G(z_A, z_A, \omega) C_2(t'). \quad (22)$$

To take into account the cavity-induced shift $\delta\omega$ of the atomic transition frequency, we make the ansatz

$$C_2(t) = e^{i\delta\omega t} \tilde{C}_2(t) \quad (23)$$

and find from Eq. (22)

$$\dot{\tilde{C}}_2(t) = -i\delta\omega \tilde{C}_2(t) - \frac{|d_{21}|^2}{\pi \hbar \epsilon_0 \mathcal{A}} \sum_k \int_0^t dt' \int_{\Delta_k} d\omega \frac{\omega^2}{c^2} \times e^{-i(\omega - \tilde{\omega}_0)(t-t')} \text{Im} G(z_A, z_A, \omega) \tilde{C}_2(t'), \quad (24)$$

where

$$\tilde{\omega}_0 = \omega_0 - \delta\omega. \quad (25)$$

Let us assume that the atomic transition frequency ω_0 is nearby a cavity resonance frequency, say ω_k , so that strong atom-field coupling may be realized. Then, the exponential $\exp[-i(\omega - \tilde{\omega}_0)(t-t')]$ can be regarded, with respect to time, as being rapidly oscillating in all the off-resonant terms with $k' \neq k$ in the sum in Eq. (24), and the time integrals in these terms can be performed in Markov approximation. That is, replacing $\tilde{C}_2(t')$ in the off-resonant terms with $\tilde{C}_2(t)$ and confining ourselves to the times large compared to Δ_k^{-1} , we may identify $\delta\omega$ with

$$\delta\omega = -\frac{|d_{21}|^2}{\pi \hbar \epsilon_0 \mathcal{A}} \sum_{k' \neq k} \int_{\Delta_{k'}} d\omega \frac{\omega^2}{c^2} \frac{\text{Im} G(z_A, z_A, \omega)}{\tilde{\omega}_0 - \omega}. \quad (26)$$

Then, from Eq. (24) we can see that $\tilde{C}_2(t)$ obeys the integro-differential equation

$$\dot{\tilde{C}}_2(t) = \int_0^t dt' \tilde{K}(t-t') \tilde{C}_2(t'), \quad (27)$$

where the kernel function $\tilde{K}(t)$ reads

$$\tilde{K}(t) = -\frac{|d_{21}|^2}{\pi \hbar \epsilon_0 \mathcal{A}} \int_{\Delta_k} d\omega \frac{\omega^2}{c^2} e^{-i(\omega - \tilde{\omega}_0)t} \text{Im} G(z_A, z_A, \omega). \quad (28)$$

In fact, Eq. (26) can only be used to calculate the \mathbf{r}_A -dependent part of the frequency shift, i. e., the cavity-induced part which arises from the scattering part of the Green function [for the decomposition of the Green function in bulk and scattering parts, see Eq. (B1)]. The \mathbf{r}_A -independent part which arises from the bulk part of the Green function and which is not cavity-specific would diverge, particularly because of the dipole approximation made. Since this part can be thought of as being already included in the definition of the transition frequency ω_0 , we can focus on the \mathbf{r}_A -dependent part. Inserting the scattering part of the Green function into Eq. (26), we derive (Appendix B)

$$\delta\omega = -\sum_{k'} \frac{\alpha_{k'}}{4|\tilde{\omega}_0 - \Omega_{k'}|^2} \times \left[\tilde{\omega}_0 \omega_{k'} - |\Omega_{k'}|^2 - \frac{\tilde{\omega}_0 \Gamma_{k'}}{4\pi} \ln\left(\frac{\omega_{k'}}{\omega_0}\right) \right] \quad (29)$$

with

$$\alpha_k = \frac{4|d_{21}|^2}{\hbar\epsilon_0\mathcal{A}|n_1(\Omega_k)|^2l} \sin^2[\omega_k|n_1(\Omega_k)|z_A/c], \quad (30)$$

where l is the length of the cavity (Fig. 1) and $n_1(\omega)$ is the (complex) refractive index of the medium inside the cavity.

To calculate the kernel function $\tilde{K}(t)$, Eq. (28), we note that, within the approximation scheme used, the frequency integration can be extended to $\pm\infty$. Employing the Green function as given by Eq. (A1) and approximating $\tilde{K}(t)$ by its leading-order contribution, we derive

$$\tilde{K}(t) = -\frac{1}{4}\alpha_k\Omega_k e^{-i(\Omega_k - \tilde{\omega}_0)t}. \quad (31)$$

Having solved Eq. (27) and calculated $\tilde{C}_2(t)$, we may eventually calculate $C_1(t)$ according to Eq. (15):

$$C_1(z, \omega, t) = \frac{d_{21}^*}{\sqrt{\pi\hbar\epsilon_0\mathcal{A}}} \frac{\omega^2}{c^2} G^*(z_A, z, \omega) \times \int_0^t dt' \sqrt{\varepsilon''(z, \omega)} \tilde{C}_2(t') e^{i(\omega - \tilde{\omega}_0)t'}. \quad (32)$$

III. QUANTUM STATE OF THE OUTGOING FIELD

For the sake of transparency, let us restrict our attention to the case where the cavity is embedded in free space. Inserting the Green tensor as given by Eq. (A1) in the one-dimensional version of Eq. (9) and decomposing the electric field outside the cavity into incoming and outgoing fields, we may represent the outgoing field, for example, at the point $z=0^+$ (cf. Fig. 1) as [43]

$$\hat{E}_{\text{out}}(z, \omega)|_{z=0^+} = i\sqrt{\frac{\hbar}{\epsilon_0\pi\mathcal{A}}} \frac{\omega^2}{c^2} \times \int dz' \sqrt{\varepsilon''(z', \omega)} G_{\text{out}}(0^+, z', \omega) \hat{f}(z', \omega), \quad (33)$$

where, according to Eq. (3), the commutation relation

$$[\hat{f}(z, \omega), \hat{f}^\dagger(z', \omega')] = \delta(\omega - \omega')\delta(z - z') \quad (34)$$

holds. For the following it will be useful to introduce the bosonic operators

$$\hat{b}_{\text{out}}(\omega) = 2\sqrt{\frac{\varepsilon_0 c \pi \mathcal{A}}{\hbar \omega}} \hat{E}_{\text{out}}(z, \omega)|_{z=0^+}. \quad (35)$$

It is not difficult to prove that

$$[\hat{b}_{\text{out}}(\omega), \hat{b}_{\text{out}}^\dagger(\omega')] = \delta(\omega - \omega'). \quad (36)$$

A. Wigner function

To calculate the quantum state of the outgoing field, we start from the multimode characteristic functional [28]

$$C_{\text{out}}[\beta(\omega), t] = \langle \psi(t) | \exp \left[\int_0^\infty d\omega \beta(\omega) \hat{b}_{\text{out}}^\dagger(\omega) - \text{H.c.} \right] | \psi(t) \rangle, \quad (37)$$

i.e., the characteristic functional of the Wigner functional. Applying the Baker–Campbell–Hausdorff formula and recalling the commutation relation (36), we may rewrite $C_{\text{out}}[\beta(\omega), t]$ as

$$C_{\text{out}}[\beta(\omega), t] = \exp \left[-\frac{1}{2} \int_0^\infty d\omega |\beta(\omega)|^2 \right] \times \langle \psi(t) | \exp \left[\int_0^\infty d\omega \beta(\omega) \hat{b}_{\text{out}}^\dagger(\omega) \right] \times \exp \left[-\int_0^\infty d\omega \beta^*(\omega) \hat{b}_{\text{out}}(\omega) \right] | \psi(t) \rangle. \quad (38)$$

Note that Eq. (38) is quite generally valid as yet.

To evaluate $C_{\text{out}}[\beta(\omega), t]$ for the state $|\psi(t)\rangle$ as given by Eq. (12), we first note that from Eq. (12) together with the commutation relation (34) and the relation $\hat{f}(z, \omega)|\{0\}\rangle = 0$ it follows that

$$\hat{f}(z, \omega)|\psi(t)\rangle = C_1(z, \omega, t) e^{-i\omega t} |1\rangle |\{0\}\rangle. \quad (39)$$

Hence, on recalling Eqs. (33) and (35), it can be seen that

$$\hat{b}_{\text{out}}(\omega)|\psi(t)\rangle = F^*(\omega, t) |1\rangle |\{0\}\rangle, \quad (40)$$

where

$$F(\omega, t) = -2i\sqrt{\frac{c}{\omega}} \frac{\omega^2}{c^2} \times \int dz \sqrt{\varepsilon''(z, \omega)} G_{\text{out}}^*(0^+, z, \omega) C_1^*(z, \omega, t) e^{i\omega t}, \quad (41)$$

with $C_1(z, \omega, t)$ being determined by Eq. (32). With the help of Eq. (35) [together with Eq. (33)] and Eq. (39), it is now not difficult to combine Eqs. (38) and (40) to obtain $C_{\text{out}}[\beta(\omega), t]$ as

$$C_{\text{out}}[\beta(\omega), t] = \exp \left[-\frac{1}{2} \int_0^\infty d\omega |\beta(\omega)|^2 \right] \times \left[1 - \left| \int_0^\infty d\omega \beta(\omega) F(\omega, t) \right|^2 \right]. \quad (42)$$

To represent $C_{\text{out}}[\beta(\omega), t]$ in a more transparent form, we introduce a time-dependent unitary transformation according to

$$\beta(\omega) = \sum_i F_i^*(\omega, t) \beta_i(t), \quad (43)$$

$$\beta_i(t) = \int_0^\infty d\omega F_i(\omega, t) \beta(\omega). \quad (44)$$

Inserting Eq. (43) in Eq. (38), we may rewrite Eq. (38) as $[C_{\text{out}}[\beta(\omega), t] \mapsto C_{\text{out}}[\beta_i(t), t]]$

$$\begin{aligned} C_{\text{out}}[\beta_i(t), t] &= \exp\left[-\frac{1}{2}\sum_i |\beta_i(t)|^2\right] \\ &\times \langle \psi(t) | \exp\left[\sum_i \beta_i(t) \hat{b}_{\text{out } i}^\dagger(t)\right] \\ &\times \exp\left[-\sum_i \beta_i^*(t) \hat{b}_{\text{out } i}(t)\right] | \psi(t) \rangle, \quad (45) \end{aligned}$$

where

$$\hat{b}_{\text{out } i}(t) = \int_0^\infty d\omega F_i(\omega, t) \hat{b}_{\text{out}}(\omega) \quad (46)$$

are the operators associated with nonmonochromatic modes $F_i(\omega, t)$ of the outgoing field, which are not yet specified. Note that

$$\hat{b}_{\text{out}}(\omega) = \sum_i F_i^*(\omega, t) \hat{b}_{\text{out } i}(t). \quad (47)$$

Accordingly, we may rewrite Eq. (42) as

$$\begin{aligned} C_{\text{out}}[\beta_i(t), t] &= \exp\left[-\frac{1}{2}\sum_i |\beta_i(t)|^2\right] \\ &\times \left[1 - \left|\sum_i \beta_i(t) \int_0^\infty d\omega F_i(\omega, t) F(\omega, t)\right|^2\right]. \quad (48) \end{aligned}$$

We now choose

$$F_1(\omega, t) = \frac{F(\omega, t)}{\sqrt{\eta(t)}}, \quad (49)$$

where, within the approximation scheme used,

$$\eta(t) = \int_0^\infty d\omega |F(\omega, t)|^2 \simeq \int_{-\infty}^\infty d\omega |F(\omega, t)|^2, \quad (50)$$

with $F(\omega, t)$ being given by Eq. (41). In this way, from Eq. (48) we obtain $C_{\text{out}}[\beta_i(t), t]$ in a 'diagonal' form with respect to the nonmonochromatic modes:

$$C_{\text{out}}[\beta_i(t), t] = C_1[\beta_1(t), t] \prod_{i \neq 1} C_i[\beta_i(t), t], \quad (51)$$

where

$$C_1(\beta, t) = e^{-|\beta|^2/2} [1 - \eta(t)|\beta|^2] \quad (52)$$

and

$$C_i(\beta, t) = e^{-|\beta|^2/2} \quad (i \neq 1). \quad (53)$$

Hence, the quantum state of the outgoing field factorizes with respect to the nonmonochromatic modes $F_i(\omega, t)$.

The Fourier transform of $C_{\text{out}}[\beta_i(t), t]$ with respect to the $\beta_i(t)$ then yields the (multi-mode) Wigner function $W_{\text{out}}(\alpha_i, t)$ sought,

$$\begin{aligned} W_{\text{out}}(\alpha_i, t) &= \frac{2}{\pi} \exp\left[-2\sum_i |\alpha_i|^2\right] [1 - 2\eta(t)(1 - 2|\alpha_1|^2)], \quad (54) \end{aligned}$$

which can be rewritten as

$$W_{\text{out}}(\alpha_i, t) = W_1(\alpha_1, t) \prod_{i \neq 1} W_i^{(0)}(\alpha_i, t), \quad (55)$$

where

$$W_1(\alpha, t) = [1 - \eta(t)]W_1^{(0)}(\alpha) + \eta(t)W_1^{(1)}(\alpha), \quad (56)$$

with $W_i^{(0)}(\alpha)$ and $W_i^{(1)}(\alpha)$, respectively, being the Wigner functions of the vacuum state and the one-photon Fock state of the i th nonmonochromatic mode. As we see, the mode labeled by the subscript $i=1$ —the excited outgoing mode—is in the mixed state described by the Wigner function $W_1(\alpha, t)$, which reveals that $\eta(t)$ can be regarded as being the efficiency to prepare the excited outgoing mode in a one-photon Fock state.

B. Continuing atom–field interaction

The formulas derived above refer to the case of continuing atom–field interaction. In particular, the efficiency $\eta(t)$ of the excited outgoing mode being prepared in a one-photon Fock state, as given by Eq. (50) together with Eq. (41), refers to this case. Its determination requires the calculation of the probability amplitude $C_1(z, \omega, t)$, which can be obtained from the probability amplitude $\tilde{C}_2(t)$ according to Eq. (32). In order to determine $\tilde{C}_2(t)$, we first substitute Eq. (31) into Eq. (27) and differentiate both sides of the resulting equation with respect to time. In this way, we derive the following second-order differential equation for $\tilde{C}_2(t)$:

$$\ddot{\tilde{C}}_2 + i(\Omega_k - \tilde{\omega}_0)\dot{\tilde{C}}_2 + \frac{1}{4}\alpha_k\Omega_k\tilde{C}_2(t) = 0, \quad (57)$$

where

$$\zeta_k \equiv \rho_k - \frac{1}{2}i\gamma_k = \sqrt{(\Omega_k - \tilde{\omega}_0)^2 + \alpha_k\Omega_k} \quad (58)$$

[with Ω_k and α_k from Eqs. (19) and (30), respectively]. The solution to Eq. (57) reads

$$\begin{aligned} \tilde{C}_2(t) &= e^{-i(\Omega_k - \tilde{\omega}_0)t/2} \\ &\times \left[\cos(\zeta_k t/2) + i \frac{\Omega_k - \tilde{\omega}_0}{\zeta_k} \sin(\zeta_k t/2) \right]. \quad (59) \end{aligned}$$

Note that when $\rho_k \gg \frac{1}{2}(\Gamma_k + \gamma_k)$, then damped vacuum Rabi oscillations of the upper-state occupation probability $|\tilde{C}_2(t)|^2 = |C_2(t)|^2$ [recall Eq. (23)] are observed (Fig. 2), where the vacuum Rabi frequency is given by $R_k = \sqrt{\alpha_k\omega_k}$.

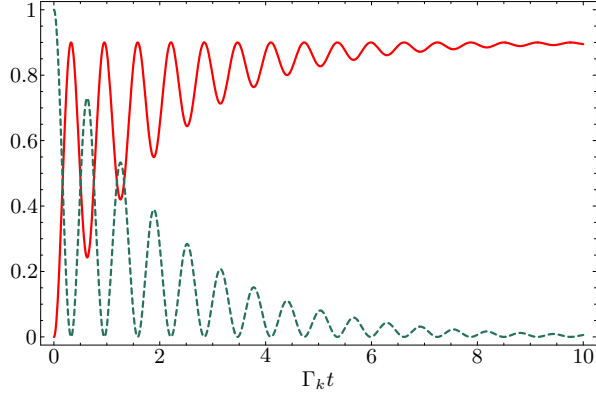


FIG. 2: The efficiency of one-photon Fock-state preparation, $\eta(t)$, Eq. (63), (solid curve) and the atomic upper-state occupation probability $|\tilde{C}_2(t)|^2$, Eq. (59), (dashed curve) are shown for $\gamma_{\text{krad}} = 0.9 \Gamma_k$, $\omega_k - \tilde{\omega}_0 = 0.1 \Gamma_k$, $R_k = 10 \Gamma_k$, $\omega_k = 2 \times 10^8 \Gamma_k$.

1. One-photon-Fock-state extraction efficiency

To calculate $\eta(t)$, we first combine Eqs. (32) and (41) to derive (Appendix D)

$$F(\omega, t) = \frac{d_{21}}{\sqrt{\pi \hbar \epsilon_0 A}} \sqrt{\frac{c}{\omega}} \frac{\omega^2}{c^2} \times \int_0^t dt' G^*(0^+, z_A, \omega) \tilde{C}_2^*(t') e^{i\omega(t-t')} e^{i\tilde{\omega}_0 t'}. \quad (60)$$

Next, we insert Eq. (59) into Eq. (60), make use of the Green function as given by Eq. (A1), and perform the t integration. Omitting off-resonant terms, we obtain

$$F(\omega, t) = \frac{\kappa_k}{2} \frac{1}{(\omega - \tilde{\omega}_0/2 - \Omega_k^*/2)^2 - \zeta_k^{*2}/4} \times \left\{ e^{i\omega t} \left[1 - e^{-i(\omega - \tilde{\omega}_0)t} C_2^*(t) \right] - \frac{i\alpha_k^* \Omega_k^* \sin(\zeta_k^* t/2)}{2\zeta_k^*} \frac{\sin(\zeta_k^* t/2)}{\omega - \Omega_k^*} e^{i(\tilde{\omega}_0 + \Omega_k^*)t/2} \right\}, \quad (61)$$

where

$$\kappa_k = -\omega_k \frac{d_{21}}{\sqrt{\pi \hbar \epsilon_0 A}} \sqrt{\frac{c}{\omega_k}} \times \frac{t_{13}^*(\Omega_k) e^{-i\omega_k n_1(\Omega_k)l/c}}{|n_1(\Omega_k)|^2 l} \sin(\omega_k |n_1(\Omega_k)| z_A/c). \quad (62)$$

In what follows we assume that $\gamma_k < \Gamma_k$. Note, that in the opposite case superstrong coupling can be observed (see, e.g., Ref. [47]). Combining Eqs. (50) and (61) and recalling Eq. (59), we arrive, after some calculation, at the following expression for the efficiency ($\gamma_k < \Gamma_k$):

$$\eta(t) = \frac{\gamma_{\text{krad}} \Gamma_k}{\Gamma_k^2 - \gamma_k^2} \frac{R_k^2}{\rho_k^2 + \Gamma_k^2/4} \left[1 - |\tilde{C}_2(t)|^2 \right], \quad (63)$$

where

$$\gamma_{\text{krad}} = \frac{c}{2|n_1(\Omega_k)|l} |T_k|^2 \quad (64)$$

with

$$T_k = \frac{t_{13}(\Omega_k)}{\sqrt{|n_1(\Omega_k)|}} e^{i\omega_k n_1(\Omega_k)l/c}. \quad (65)$$

In particular in the limit when $t \rightarrow \infty$, then $\eta(t) \rightarrow [\gamma_{\text{krad}} \Gamma_k / (\Gamma_k^2 - \gamma_k^2)] [R_k^2 / (\rho_k^2 + \Gamma_k^2/4)]$, which approximately simplifies to $\eta(t) \rightarrow \gamma_{\text{krad}} / \Gamma_k$ for a sufficiently high- Q cavity and almost exact resonance. Note that this value is always observed at the instants when the atom is in the lower state. The behavior of the function $\eta(t)$ is illustrated in Fig. 2. For comparison, the atomic upper-state occupation probability $|\tilde{C}_2(t)|^2$ is also shown.

2. Shape of the excited outgoing field

To study the propagation of the excited outgoing field in space and time, we consider the operator of the electric field strength

$$\hat{E}_{\text{out}}^{(+)}(z) = \int_0^\infty d\omega e^{i\omega z/c} \hat{E}_{\text{out}}(z, \omega) \Big|_{z=0_+} \quad (66)$$

($z > 0$). Recalling Eq. (35), we may write

$$\hat{E}_{\text{out}}^{(+)}(z) = \frac{1}{2} \int_0^\infty d\omega \sqrt{\frac{\hbar \omega}{\epsilon_0 c \pi A}} e^{i\omega z/c} \hat{b}_{\text{out}}(\omega) \quad (67)$$

or equivalently, inserting Eq. (47) into Eq. (67),

$$\hat{E}_{\text{out}}^{(+)}(z) = \sum_i \phi_i^*(z, t) \hat{b}_{\text{out}i}(t), \quad (68)$$

where

$$\phi_i(z, t) = \frac{1}{2} \int_0^\infty d\omega \sqrt{\frac{\hbar \omega}{\epsilon_0 c \pi A}} e^{-i\omega z/c} F_i(\omega, t). \quad (69)$$

The intensity of the outgoing field at position z is then determined by

$$I(z, t) = \langle \psi(t) | \hat{E}_{\text{out}}^{(-)}(z) \hat{E}_{\text{out}}^{(+)}(z) | \psi(t) \rangle \quad (70)$$

with $\hat{E}_{\text{out}}^{(+)}(z)$ and $\hat{E}_{\text{out}}^{(-)}(z) = [\hat{E}_{\text{out}}^{(+)}(z)]^\dagger$ from Eq. (68). Using Eqs. (46), (40), (49), and (72), we derive

$$I(z, t) = \eta(t) |\phi_1(z, t)|^2, \quad (71)$$

which reveals that $\phi_1(z, t)$ represents the spatio-temporal shape of the outgoing field associated with the excited mode $F_1(\omega, t)$, and $\eta(t)$ is nothing but the expectation value $\langle \psi(t) | \hat{b}_{\text{out}1}^\dagger(t) \hat{b}_{\text{out}1}(t) | \psi(t) \rangle$.

For simplicity, let us restrict our attention to the case where the cavity is not filled with medium ($n_1 \equiv 1$) and assume that the thickness of the fractionally transparent

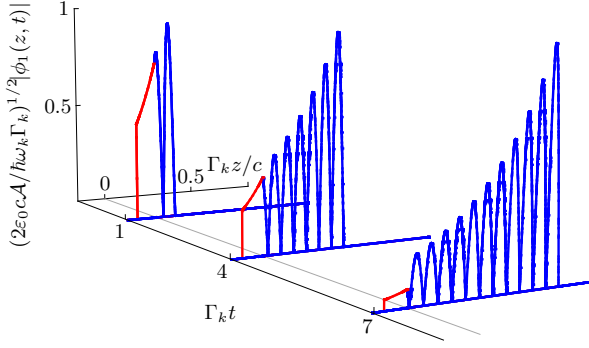


FIG. 3: The spatio-temporal behavior of the excited outgoing wave packet, $|\phi_1(z, t)|$, Eq. (73), in the case of continuing atom–field interaction for $\Gamma_k l/c = 0.7$. The parameters are the same as in Fig. 2.

mirror is small compared with the cavity length. Then, as shown in Appendix E, $\phi_1(z, t)$ can be regarded as also describing the part of the excited outgoing wave packet that may be still inside the cavity, i. e., $-l \leq z < 0$. Hence, we may write

$$\begin{aligned} \phi_1(z, t) &= \Theta(z+l) \frac{1}{2} \int_0^\infty d\omega \sqrt{\frac{\hbar\omega}{\varepsilon_0 c \pi \mathcal{A}}} e^{-i\omega z/c} F_1(\omega, t) \\ &\simeq \Theta(z+l) \frac{1}{2} \sqrt{\frac{\hbar\omega_k}{\varepsilon_0 c \pi \mathcal{A}}} \int_0^\infty d\omega e^{-i\omega z/c} F_1(\omega, t), \end{aligned} \quad (72)$$

which, by means of Eqs. (49) and (61), can be evaluated to (approximately) yield

$$\begin{aligned} \phi_1(z, t) &= \Theta(-z)\Theta(z+l)\phi_1^<(z, t) \\ &\quad - \Theta(z)\Theta(ct-z)\phi_1^>(z, t), \end{aligned} \quad (73)$$

where

$$\begin{aligned} \phi_1^>(z, t) &= \sqrt{\frac{\pi \hbar \omega_k}{\varepsilon_0 c \mathcal{A} \eta(t)}} \frac{\kappa_k}{\zeta_k^*} e^{i(\tilde{\omega}_0 + \Omega_k^*)(t-z/c)/2} \\ &\quad \times \sin[\zeta_k^*(t-z/c)/2] \end{aligned} \quad (74)$$

and

$$\begin{aligned} \phi_1^<(z, t) &= \sqrt{\frac{\pi \hbar \omega_k}{\varepsilon_0 c \mathcal{A} \eta(t)}} \frac{\kappa_k}{\zeta_k^*} e^{i\Omega_k^*(t-z/c)} \\ &\quad \times e^{i(\tilde{\omega}_0 - \Omega_k^*)t/2} \sin(\zeta_k^* t/2). \end{aligned} \quad (75)$$

However note that in Eq. (68) describing the outgoing field outside as well as inside the cavity, the outside- and inside-parts of $\phi_i(z, t)$ are in general associated with different operators $\hat{b}_{\text{out } i}(t)$, because of absorption in the fractionally transparent mirror.

The behavior of the absolute value of $\phi_1(z, t)$ as a function of t and z is illustrated in Fig. 3. Comparison with Fig. 2 reveals that $|\phi_1^>(z, t)|$ oscillates according to the

Rabi frequency of the atom–field interaction. It should be stressed that in Eq. (51) the argument $\beta_1(t)$ of the characteristic function $C_1[\beta_1(t), t]$ of the quantum state of the excited outgoing mode $F_1(\omega, t)$ refers to the wave packet $\phi_1(z, t)$ as a whole, i. e., it refers not only to its part outside the cavity but also to its part inside the cavity, which is observed for short times ($\Gamma_k t \lesssim 1$) when the emitted photon belongs to the cavity and the world outside the cavity simultaneously.

C. Short-term atom–field interaction

Let us now consider the case where the atom leaves the cavity at some finite time τ so that the interaction of the atom with the cavity-assisted field effectively terminates at this time. Whereas for times t in the interval $0 \leq t \leq \tau$, the state vector $|\psi(t)\rangle$ is again given by Eq. (12), it reads

$$|\psi(t)\rangle = e^{-i(t-\tau)\hat{H}_0/\hbar} |\psi(\tau)\rangle \quad (76)$$

if $t \geq \tau$. Here, \hat{H}_0 is the Hamiltonian of the uncoupled system, i. e., the sum of the first two terms in Eq. (11), and $|\psi(\tau)\rangle$ is given by $|\psi(t)\rangle$ from Eq. (12) for $t = \tau$. Hence, Eq. (76) can be written as ($t \geq \tau$)

$$\begin{aligned} |\psi(t)\rangle &= C_2(\tau) e^{-i\omega_0 t} |2\rangle |0\rangle \\ &\quad + \int dz \int_0^\infty d\omega C_1(z, \omega, \tau) e^{-i\omega t} |1\rangle \hat{f}^\dagger(z, \omega) |0\rangle. \end{aligned} \quad (77)$$

Note that the condition $\rho_k \tau \gg 1$ is required in order to observe damped vacuum Rabi oscillations.

1. One-photon-Fock-state extraction efficiency

To calculate the quantum state of the outgoing field in the case of short-term atom–field interaction, we insert Eq. (77) in Eq. (37) and use Eq. (35) together with Eq. (33). In this way, we again arrive at Eq. (48), but now with

$$\begin{aligned} F(\omega, t, \tau) &= -2i \sqrt{\frac{c}{\omega}} \frac{\omega^2}{c^2} \\ &\quad \times \int dz' \sqrt{\varepsilon''(z', \omega)} G_{\text{out}}^*(0^+, z', \omega) C_1^*(z', \omega, \tau) e^{i\omega t} \end{aligned} \quad (78)$$

in place of $F(\omega, t)$. Comparing Eq. (78) with Eq. (41), we easily see that

$$F(\omega, t, \tau) = e^{i\omega(t-\tau)} F(\omega, \tau). \quad (79)$$

Choosing $[F_i(\omega, t) \mapsto F_i(\omega, t, \tau)]$

$$F_1(\omega, t, \tau) = \frac{F(\omega, t, \tau)}{\sqrt{\eta(t, \tau)}}, \quad (80)$$

we are again left with an equation of the form of Eq. (51) [together with Eqs. (52) and (53)], where, according to

Eq. (50) [$\eta(t) \mapsto \eta(t, \tau)$], the efficiency of preparation of the excited outgoing mode in a one-photon Fock state now reads

$$\eta(t, \tau) = \int_0^\infty d\omega |F(\omega, t, \tau)|^2 = \eta(\tau). \quad (81)$$

Hence, $\eta(t, \tau)$ does not depend on t ; it is simply given by the efficiency observed in the case of continuing atom-field interaction at time τ , i. e., by $\eta(t)$ from Eq (50) for $t = \tau$.

2. Shape of the excited outgoing field

A calculation in line with that leading from Eq. (66) to Eq. (73), now yields the following form of the excited outgoing mode [$\phi(z, t) \mapsto \phi(z, t, \tau)$]:

$$\begin{aligned} \phi_1(z, t, \tau) = & \Theta(ct - c\tau - z)\Theta(z + l)\phi_1^<(z, t, \tau) \\ & + \Theta(z - ct + c\tau)\Theta(ct - z)\phi_1^>(z, t, \tau), \end{aligned} \quad (82)$$

where

$$\begin{aligned} \phi_1^>(z, t, \tau) = & \sqrt{\frac{\pi\hbar\omega_k}{\varepsilon_0 c \mathcal{A} \eta(t)} \frac{\kappa_k}{\zeta_k^*}} e^{i(\tilde{\omega}_0 + \Omega_k^*)(t-z/c)/2} \\ & \times \sin[\zeta_k^*(t - z/c)/2] \end{aligned} \quad (83)$$

and

$$\begin{aligned} \phi_1^<(z, t, \tau) = & \sqrt{\frac{\pi\hbar\omega_k}{\varepsilon_0 c \mathcal{A} \eta(t)} \frac{\kappa_k}{\zeta_k^*}} e^{i\Omega_k^*(t-z/c)} \\ & \times e^{i(\tilde{\omega}_0 - \Omega_k^*)\tau/2} \sin(\zeta_k^*\tau/2). \end{aligned} \quad (84)$$

Note that Eq. (83) agrees with Eq. (74). The behavior of the absolute value of $\phi_1(z, t, \tau)$ is illustrated in Fig. 4, where the interaction time τ is chosen in such a way that it is the time at which the atom is the first time in the

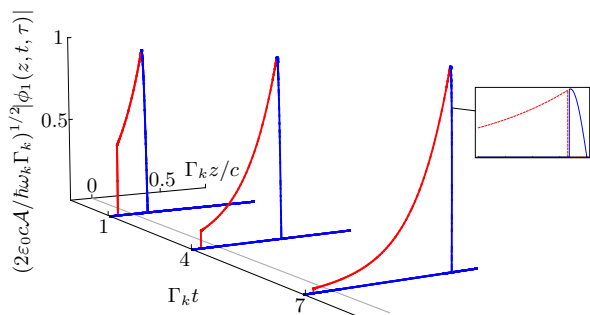


FIG. 4: The spatio-temporal behavior of the excited outgoing wave packet $|\phi_1(z, t, \tau)|$, Eq. (82), in the case of short-term atom-field interaction for $\Gamma_k \tau = 0.3$, $\Gamma_k l/c = 0.7$. The parameters are the same as in Fig. 2. The inset shows the leading edge (solid curve) and the trailing edge (dashed curve).

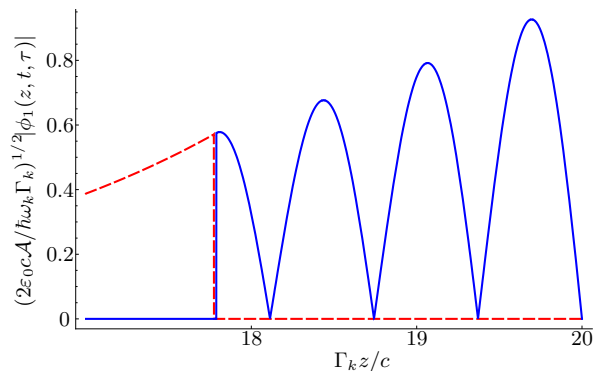


FIG. 5: The spatio-temporal shape of the excited outgoing mode, $|\phi_1(z, t, \tau)|$, Eq. (82), for $\Gamma_k \tau = 2.2$, $\Gamma_k t = 20$, and $\Gamma_k l/c = 0.7$. The parameters are the same as in Fig. 2. The solid (dashed) curve shows the leading (trailing) edge.

lower state (cf. the upper-state occupation probability shown in Fig. 2).

We see that the excited outgoing field has, for the chosen interaction times τ , the form of a single-peaked pulse, whose trailing and leading edges are determined by $\phi_1^<(z, t, \tau)$ and $\phi_1^>(z, t, \tau)$, respectively. Since $\phi_1^>(z, t, \tau)$ approaches zero as τ tends to zero, the pulse can be regarded as being fully determined by $\phi_1^<(z, t, \tau)$ for sufficiently short interaction times. The situation can drastically change when longer interaction times are considered so that τ cannot be regarded as being small compared to Γ_k^{-1} . In this case, the contribution to $\phi_1(z, t, \tau)$ of $\phi_1^>(z, t, \tau)$ can become the dominating one, and, if the atom is allowed to undergo Rabi oscillations before it leaves the cavity, a multi-peaked pulse is observed, as can be seen from Fig. 5.

D. Comparison with quantum noise theories

Let us compare the results with the ones obtained by using methods of QNT. As QNT is based on the assumption that the electromagnetic fields inside and outside the cavity represent independent degrees of freedom, which give rise to two separate Hilbert spaces, there is in particular no way to consider (excited) outgoing modes that simultaneously belong to the cavity and the outside world. To go into more details, let us first consider the regime of continuing atom-field interaction.

1. Continuing atom-field interaction

To describe the excited outgoing field inside and outside the cavity from the point of view of QNT, one could consider wave packets of the types of $\phi_1^>(z, t)$ [Eq. (74)] and $\phi_1^<(z, t)$ [Eq. (75)], respectively, and introduce func-

tions $F_1^>(\omega, t)$ and $F_1^<(\omega, t)$ according to

$$F_1^{>(<)}(\omega, t) = \frac{1}{\sqrt{2\pi c \mathcal{N}_1^{>(<)}(t)}} \int_{>(<)} dz e^{i\omega z/c} \phi_1^{>(<)}(z, t), \quad (85)$$

where

$$\mathcal{N}_1^{>(<)}(t) = \int_{>(<)} dz |\phi_1^{>(<)}(z, t)|^2. \quad (86)$$

Here, the integral $\int_{>(<)} dz \dots$ runs over the interval $0 < z < ct$ ($-l < z < 0$). Now, one could identify $F_1(\omega, t)$ in Eq. (48) for $C_{\text{out}}[\beta_i(t), t]$ with $F_1^>(\omega, t)$. Since for the field inside the cavity, Eq. (48) must be replaced by Eq. (E11), one could also identify $F_1(\omega, t)$ with $F_1^<(\omega, t)$. Disregarding the ‘interference’ terms, which prevent $C_{\text{out}}[\beta_i(t), t]$ from being a product, one may introduce the single-mode characteristic function

$$C_1^{>(<)}(\beta, t) = e^{-|\beta|^2/2} \left[1 - \eta^{>(<)}(t) |\beta|^2 \right] \quad (87)$$

together with

$$\eta^{>(<)}(t) = \left| \int_0^\infty d\omega F_1^{>(<)}(\omega, t) F_1^{>(<)*}(\omega, t) \right|^2, \quad (88)$$

where, according to Eqs. (48) and (E11), respectively,

$$F^>(\omega, t) = F(\omega, t) \quad (89)$$

and

$$F^<(\omega, t) = \sqrt{\frac{\Gamma_k}{\gamma_{\text{krad}}}} F(\omega, t). \quad (90)$$

Obviously, Eq. (87) together with Eq. (88) replaces Eq. (52) together with Eq. (50). Using Eqs. (49), (72), (85), (85), and (86), after some calculations we find that $\eta^{>(<)}(t)$ can be written as

$$\eta^>(t) = \frac{2\varepsilon_0 \mathcal{A}}{\hbar\omega_k} \eta(t) \mathcal{N}_1^>(t), \quad (91)$$

$$\eta^<(t) = \frac{\Gamma_k}{\gamma_{\text{krad}}} \frac{2\varepsilon_0 \mathcal{A}}{\hbar\omega_k} \eta(t) \mathcal{N}_1^<(t), \quad (92)$$

with $\eta(t)$ from Eq. (50).

To give a physical explanation of Eqs. (91) and (92), we first note that from Eq. (71) it follows that

$$I^>(t) = \int_{>} dz I(z, t) = \eta^>(t). \quad (93)$$

From the theory of photodetection of light [36] we know that the probability of registering a photon during the time interval $[0, t]$ by a detector at $z=0_+$ is proportional to $I^>(t)$. Hence, the quantity $\eta^>(t)$, which refers to the part of the excited outgoing wave packet that is quite outside the cavity, cannot be regarded, in general, as being

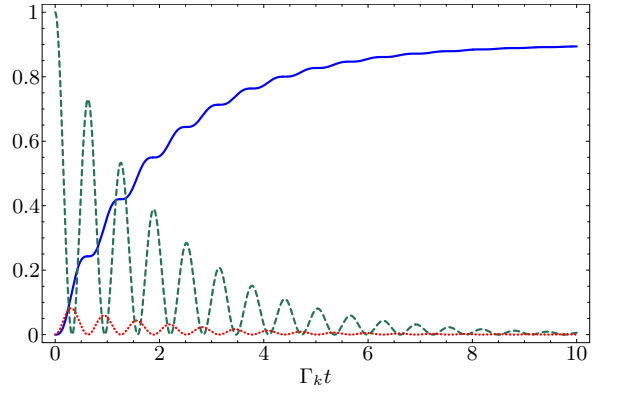


FIG. 6: The quantities $\eta^>(t)$ (solid curve) and $\eta^<(t)$ (dotted curve), c.f. Eqs. (91) and (92) ($\Gamma_k l/c=0.7$), and the atomic upper-state occupation probability $|\tilde{C}_2(t)|^2$, Eq. (59), (dashed curve). The parameters are the same as in Fig. 2.

the efficiency of preparation of the outgoing field in a one-photon Fock-state; it can be merely regarded as being proportional to the probability of registering an emitted photon outside the cavity during the chosen time interval. To clarify the meaning of the quantity $\eta^<(t)$, which refers to the part of the excited outgoing wave packet that is quite inside the cavity, we recall that the total excited field inside the cavity consists of a part traveling from the left to the right and a part traveling from the right to the left. Obviously, $\eta^<(t)$ refers to the (small) fraction of the former part which is transmitted through the fractionally transparent mirror. It is hence proportional to the probability of registering a photon if this fraction of the part of the excited field inside the cavity which travels from the left to the right could be detected. The dependence on t of $\eta^>(t)$ and $\eta^<(t)$ is illustrated in Fig. 6. As we can see, $\eta^>(t)$ almost monotonically increases with time, while $\eta^<(t)$ decreases with increasing time in an oscillatory manner. As expected, $\eta^>(t)$ approaches $\eta(t)$ as $\Gamma_k t$ tends to infinity (cf. Fig. 2). Clearly, in the limit when $\Gamma_k t \rightarrow \infty$, the wave packet $\phi_1(z, t)$ associated with the excited outgoing mode $F_1(\omega, t)$ is strictly localized outside the cavity and $C_1^>(\beta, t)$ equals the characteristic function $C_1(\beta, t)$ of the quantum state of the excited outgoing mode.

Since the wave packet associated with the excited outgoing mode covers the areas inside and outside the cavity in general, a photon carried by the mode belongs simultaneously to the two areas in general. To model this effect within the framework of QNT, where the fields inside and outside the cavity are considered as belonging to two different Hilbert spaces, one had to introduce (on disregarding absorption losses) entangled states between a photon inside the cavity and a photon outside the cavity. Needless to say that from the point of view of QED, such a concept would be rather artificial.

2. Short-term atom–field interaction

Let us compare the results with the ones in Ref. [43], where—in analogy to QNT—cavity modes are explicitly introduced and, on this basis, input–output relations are derived. In particular, let us consider a single excited cavity mode, say the k th mode, and assume that at initial time $t=0$ this mode is prepared in an excited state and the field outside the cavity is in the vacuum state. This means that the time of preparation of the mode in the excited state (which corresponds to the time τ of the atom–field interaction in Sec. III C) must be much smaller than its decay time Γ_k^{-1} . In the frequency interval Δ_k , the operator input–output relation in the Heisenberg picture can then be written as [43]

$$\hat{b}_{\text{kout}}(\omega, t) = F_{\text{krel}}^*(\omega, t)\hat{a}_k(0) + \hat{B}_k(\omega, t), \quad (94)$$

where $\hat{a}(0)$ is the photon destruction operator of the cavity mode at the initial time, $\hat{B}_k(\omega, t)$ is a linear functional of the operators of the input field $\hat{b}_{\text{kin}}(\omega, 0)$ and the noise sources $\hat{c}_{k\lambda}(\omega, 0)$ both taken at the initial time (see Appendix F), and

$$F_{\text{krel}}(\omega, t) = \frac{i}{\sqrt{2\pi}} \left[\frac{c}{2n_1(\Omega_k)l} \right]^{\frac{1}{2}} T_k^* e^{i\omega t} \times \frac{\exp[-i(\omega - \Omega_k^*)(t + \Delta t)] - 1}{\omega - \Omega_k^*} \quad (95)$$

($\Delta t \rightarrow 0_+$). From Eq. (94) one can conclude that $F_{\text{krel}}(\omega, t)$ represents the part of the output field relevant to the excited cavity mode. The efficiency to find at time t this part—referred to as the relevant (non-monochromatic) output mode—in a one-photon Fock state when the cavity mode has initially been prepared in a one-photon Fock state then reads as [43]

$$\eta_{\text{krel}}(t) = \int_0^\infty d\omega |F_{\text{krel}}(\omega, t)|^2 \simeq \frac{\gamma_{\text{krad}}}{\Gamma_k} [1 - e^{-\Gamma_k t}], \quad (96)$$

which is seen to be time dependent, in contrast to the time-independent efficiency (81).

This result is not surprising, since—in contrast to the relevant mode, which by construction defines a wave packet entirely outside the cavity—the outgoing wave packet $\phi_1(z, t, \tau)$ [Eq. (82)], which corresponds to the excited mode that really carries the photon, covers simultaneously the areas inside and outside the cavity (cf. Fig. 4). As in the case of continuing atom–field interaction, it is natural to expect that only in the case when the condition $\Gamma_k t \gg 1$ holds, then $\eta_{\text{krel}}(t) \simeq \eta(\tau)$ for a value of τ for which the atom is in the ground state.

Returning to Sec. III C, let us now consider the leading edge of $\phi_1(z, t, \tau)$ and that part of the trailing edge of $\phi_1(z, t, \tau)$ which is entirely outside the cavity, and, in

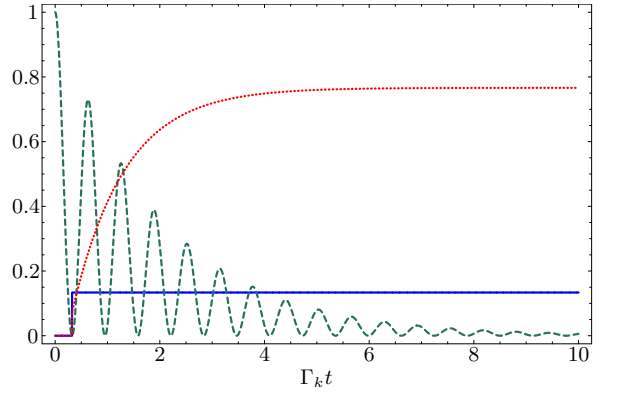


FIG. 7: The quantities $\eta^>(t, \tau)$ (solid curve) and $\eta^<(t, \tau)$ (dotted curve), Eq. (101), and the atomic upper-state occupation probability $|\tilde{C}_2(t)|^2$, Eq. (59), (dashed curve) for $\Gamma_k \tau = 0.3$, $\Gamma_k l/c = 0.7$. The parameters are the same as in Fig. 2.

line with Eq. (85), introduce the functions ($t \geq \tau$)

$$F_1^{>(<)}(\omega, t, \tau) = \frac{1}{\sqrt{2\pi c \mathcal{N}_1^{>(<)}}(t, \tau)} \times \int_{>(<)} dz e^{i\omega z/c} \phi_1^{>(<)}(z, t, \tau), \quad (97)$$

where $\int_{>(<)} dz \dots$ runs over the interval $c(t - \tau) < z < ct$ [$0 < z < c(t - \tau)$], and

$$\mathcal{N}_1^{>(<)}}(t, \tau) = \int_{>(<)} dz |\phi_1^{>(<)}}(z, t, \tau)|^2, \quad (98)$$

so that, in view of QNT, a characteristic function of the form of Eq. (87) could be defined, with $\eta^{>(<)}}(t)$ being replaced by

$$\eta^{>(<)}}(t, \tau) = \left| \int_0^\infty d\omega F_1^{>(<)}}(\omega, t, \tau) F^*(\omega, t, \tau) \right|^2. \quad (99)$$

Straightforward calculation, using Eqs. (97) and (98) together with Eqs. (72), (80), and (82), yields

$$\eta^{>(<)}}(t, \tau) = \frac{2\varepsilon_0 \mathcal{A}}{\hbar \omega_k} \eta(\tau) \mathcal{N}_1^{>(<)}}(t, \tau). \quad (100)$$

In particular,

$$\eta^<(t, \tau) = \frac{R_k^2}{|\zeta_k|^2} |\sin(\zeta_k \tau/2)|^2 e^{-\Gamma_k \tau/2} \eta_{\text{krel}}(t - \tau), \quad (101)$$

with $\eta_{\text{krel}}(t)$ according to Eq. (96). The behavior of $\eta^>(t, \tau)$ and $\eta^<(t, \tau)$ as functions of t is illustrated in Fig. 7. To make contact with the results in Ref. [43], we assume strong atom–field coupling, almost exact resonance, $R_k^2/|\zeta_k|^2 \simeq 1$, and short interaction time, such that $\Gamma_k \tau \ll 1$ as well as $|\sin(\zeta_k \tau/2)|^2 \simeq 1$,

i.e., $|\tilde{C}_2(\tau)|^2 \simeq 0$. In this limiting case we have $\eta^<(t, \tau) \simeq \eta_{k\text{rel}}(t)$. Recalling, that when $\Gamma_k \tau \ll 1$, then the contribution of the leading edge $\phi_1^>(t, \tau)$ to $\phi_1(t, \tau)$ can be neglected, $\phi_1^<(t, \tau) \simeq \phi_1(t, \tau)$, we conclude that $\eta_{k\text{rel}}(t) \simeq \eta(\tau)$ if $\Gamma_k t \gg 1$. From reasons similar to those applied to the case of continuing atom–field interaction it follows that $\eta^<(t, \tau) \simeq \eta_{k\text{rel}}(t)$ cannot be regarded, in general, as being the efficiency of preparation of the outgoing field in a single-photon Fock-state; it may be merely regarded as being the probability of detection of a photon outside the cavity.

Finally, let us address the following point. In QNT it is commonly assumed that (at equal times) input-field and cavity-field variables commute. On the other hand, the QED approach in Ref. [43] shows that

$$\left[\hat{a}_k, \hat{b}_{\text{kin}}^\dagger(\omega) \right] = F_k(\omega), \quad (102)$$

where

$$F_k(\omega) = \sqrt{\frac{c}{2l}} \sqrt{\frac{\Gamma_k}{\gamma_{k\text{rad}}}} \frac{T_k}{\sqrt{2\pi}} \frac{i}{\omega - \Omega_k}. \quad (103)$$

Hence the question rises of whether or not the commutator in Eq. (102) can be effectively set equal to zero.

To give an answer, we introduce the nonmonochromatic input mode that is related to this commutator,

$$\hat{b}_{\text{kin}}(t) = \int_0^\infty d\omega F_{\text{kin}}(\omega, t) \hat{b}_{\text{kin}}(\omega), \quad (104)$$

where

$$F_{\text{kin}}(\omega, t) = F_k(\omega) e^{-i\omega t}. \quad (105)$$

Using Eq. (94) together with the formulas in Appendix F, one can calculate the corresponding nonmonochromatic mode of the output field,

$$F_{k\text{out}}(\omega, t) = \frac{r_{31}^*(\omega)}{|r_{31}(\omega)|} F_k(\omega) e^{i\omega t}, \quad (106)$$

and show that

$$\begin{aligned} & \int_0^\infty d\omega F_{k\text{rel}}^*(\omega, t) F_{k\text{out}}(\omega, t) \\ & \simeq \int_{-\infty}^\infty d\omega F_{k\text{rel}}^*(\omega, t) F_{k\text{out}}(\omega, t) = 0. \end{aligned} \quad (107)$$

Hence, the relevant output mode as defined by Eq. (95) is not related to the commutator in question. Applying Eq. (72) to the functions $F_{k\text{rel}}(\omega, t)$, Eq. (95), and $F_{k\text{out}}(\omega, t)$, Eq. (106), one can calculate the corresponding spatio-temporal shapes

$$\phi_{k\text{rel}}(z, t) = -\Theta(z)\Theta(ct - z) \frac{1}{2} \sqrt{\frac{\hbar\omega_k}{\varepsilon_0 l \mathcal{A}}} T_k^* e^{i\Omega_k^*(t-z/c)} \quad (108)$$

and

$$\begin{aligned} \phi_{k\text{com}}(z, t) &= \Theta(z - ct) \\ &\times \frac{1}{2} \sqrt{\frac{\hbar\omega_k}{\varepsilon_0 l \mathcal{A}}} \sqrt{\frac{\Gamma_k}{\gamma_{k\text{rad}}}} \frac{r_{31}^*(\Omega_k)}{|r_{31}(\Omega_k)|} T_k e^{i\Omega_k(t-z/c)}, \end{aligned} \quad (109)$$

respectively. Comparing Eqs. (108) and (109) with Eq. (82), we see that, as expected, $\phi_{k\text{rel}}(z, t)$ matches, for $\Gamma_k \tau \ll 1$, that part of $\phi_1(z, t, \tau) \simeq \phi_1^<(z, t, \tau)$ which is entirely outside the cavity, whereas $\phi_{k\text{com}}(z, t)$ does not contribute to $\phi_1(z, t, \tau)$. We are thus left with the result that when the interaction time is sufficiently short, then the commutator in question can be effectively set equal to zero in the scheme under consideration.

IV. SUMMARY AND CONCLUDING REMARKS

Within the frame of macroscopic QED in dispersing and absorbing media, we have given an exact description of the resonant interaction of a two-level atom in a high- Q cavity with the cavity-assisted electromagnetic field, with the atom and the field being initially in the upper state and the ground state, respectively. Using a source-quantity representation of the electromagnetic field, we have performed the calculations for a one-dimensional cavity bounded by a perfectly reflecting and a fractionally transparent mirror, without regarding the fields inside and outside the cavity as representing independent degrees of freedom. We have applied the theory to the determination of (i) the Wigner function of the quantum state of the excited outgoing mode and (ii) the spatio-temporal shape of the wave packet corresponding to this mode.

As expected, the quantum state of the excited outgoing mode is always a mixture of a one-photon Fock state and the vacuum state, because of the unavoidable unwanted losses. In the case of continuing atom–field interaction, the efficiency of the mode being prepared in a one-photon Fock state is time dependent and features Rabi oscillation in the regime of strong atom–field coupling. This is due to the fact that, for not too long times, the corresponding wave packet covers the areas both inside and outside the cavity so that a photon emitted by the atom belongs simultaneously to the two areas and can thus be reabsorbed by the atom. In particular, from the part of the wave packet that is entirely localized outside the cavity, the probability of registering the emitted photon by a photodetector placed outside the cavity can be calculated—a quantity which, as expected, monotonously increases with time and approaches the efficiency of one-photon Fock-state preparation in the long-time limit.

In the case of short-term atom–field interaction, where the atom leaves the cavity at some interaction time τ , the efficiency of the excited outgoing mode being prepared in a one-photon Fock state is constant for all times

$t \geq \tau$. It is simply given by the value of the efficiency observed at time $t = \tau$ in the case of continuing atom–field interaction. This result again reflects the fact that the field associated with the excited outgoing mode covers the areas both inside and outside the cavity. In particular, if the atom leaves the cavity when it is the first time in the ground state, then this field can be regarded as a single-peak pulse, the trailing edge of which covers the two areas. Moreover, when the interaction time is sufficiently short, then the pulse can be approximated by its trailing edge, whose part that is entirely localized outside the cavity matches the field determined by the relevant mode appearing in the input–output relations derived within the frame of QNT. Again, the part of the excited outgoing field that is entirely localized outside the cavity only determines the probability of registering the emitted photon by a photodetector placed outside the cavity and not the efficiency of one-photon Fock-state preparation in general.

The results particularly imply that the efficiency of preparing the outgoing field in a one-photon Fock state, as suggested from QNT, is in fact proportional to the probability of registering a photon outside the cavity. Only in the long-time limit the two quantities become identical. As in QNT or related approaches to cavity QED modes that simultaneously cover the areas inside and outside a cavity are a priori excluded from consideration, effects associated with modes of this type cannot be exactly described by such methods. What one could do to is to model them by introducing—somewhat artificially from the point of view of QED—entangled states where a photon inside the cavity is entangled with a photon outside the cavity.

The results also show that in the short-time limit when the leading edge of the excited outgoing field can be disregarded, then the commutator in Ref. [43] between the input field and the cavity field at equal times can be effectively set zero, in agreement with the QNT postulate. As we can see from Fig. 5, the contribution to the outgoing mode which corresponds to the leading edge increases with the atom–field interaction time. In practice this time can be comparable with the time of extraction of the state from the cavity (see, e. g., the scheme in Ref. [22])—a case which with respect to more complicated schemes, which may contain pumped multi-level atoms and/or excited input fields, requires further studies.

Acknowledgments

This work was supported by the Deutsche Forschungsgemeinschaft. C.D.F. thanks Thomas Richter for useful discussions.

APPENDIX A: MULTILAYER PLANAR STRUCTURE

The one-dimensional cavity is modeled by a planar multilayer system, where the layers $j = 0$ and $j = 2$, respectively, are assumed to correspond to perfectly and fractionally reflecting mirrors, which confine the cavity whose interior space corresponds to the layer $j = 1$. With respect to the cavity axis z , we use shifted coordinates such that $0 < z < l$ for $j = 1$, $0 < z < d$ for $j = 2$, and $0 < z < \infty$ for $j = 3$. The (one-dimensional) Green function in the frequency domain reads [48]

$$G^{(jj')}(z, z', \omega) = \frac{1}{2}i[\mathcal{E}^{(j)>}(z, \omega)\Xi^{jj'}\mathcal{E}^{(j')<}(z', \omega)\Theta(j - j') + \mathcal{E}^{(j)<}(z, \omega)\Xi^{j'j}\mathcal{E}^{(j')>}(z', \omega)\Theta(j' - j)], \quad (\text{A1})$$

where the functions

$$\mathcal{E}^{(j)>}(z, \omega) = e^{i\beta_j(\omega)(z-d_j)} + r_{j/3}(\omega)e^{-i\beta_j(\omega)(z-d_j)} \quad (\text{A2})$$

and

$$\mathcal{E}^{(j)<}(z, \omega) = e^{-i\beta_j(\omega)z} + r_{j/0}(\omega)e^{i\beta_j(\omega)z}, \quad (\text{A3})$$

respectively, represent waves of unit strength traveling rightward and leftward in the j th layer and being reflected at the boundary [note that $\Theta(j - j')$ means $\Theta(z - z')$ for $j = j'$]. Further, $\Xi^{jj'}$ is defined by

$$\Xi^{jj'} = \frac{1}{\beta_3(\omega)t_{0/3}(\omega)} \frac{t_{0/j}(\omega)e^{i\beta_j(\omega)d_j}}{D_j(\omega)} \frac{t_{3/j'}(\omega)e^{i\beta_{j'}(\omega)d_{j'}}}{D_{j'}(\omega)}, \quad (\text{A4})$$

where

$$D_j(\omega) = 1 - r_{j/0}(\omega)r_{j/3}(\omega)e^{2i\beta_j(\omega)d_j} \quad (\text{A5})$$

and

$$\beta_j(\omega) = \sqrt{\varepsilon_j(\omega)} \frac{\omega}{c} = [n'_j(\omega) + in''_j(\omega)] \frac{\omega}{c} \quad (\text{A6})$$

($d_1 = l$, $d_2 = d$, $d_3 = 0$). The quantities $t_{j/j'}(\omega) = [\beta_j(\omega)/\beta_{j'}(\omega)]t_{j'/j}(\omega)$ and $r_{j/j'}(\omega)$ denote, respectively, the transmission and reflection coefficients between the layers j' and j , which can be recursively determined. Note that the zeros of the function $D_1(\omega)$ [Eq. (A5) for $j = 1$ and $r_{10} = -1$] determine the (complex) resonance frequencies Ω_k of the cavity under consideration,

$$D_1(\Omega_k) = 1 + r_{13}(\Omega_k)e^{2i\beta_1(\Omega_k)l} = 0. \quad (\text{A7})$$

In particular, the part of the Green function that relates the outgoing field at z to the sources at z' in the j' th layer is given by

$$G_{\text{out}}(z, z', \omega) \equiv G_{\text{out}}^{(3j')}(z, z', \omega) = G^{(3j')}(z, z', \omega) - G_{\text{in}}^{(3j')}(z, z', \omega), \quad (\text{A8})$$

where

$$G_{\text{in}}^{(3j')}(z, z', \omega) = \frac{1}{2\beta_3(\omega)} ie^{-i\beta_3(\omega)z} e^{i\beta_{j'}(\omega)z'} \Theta(z' - z). \quad (\text{A9})$$

APPENDIX B: DERIVATION OF EQ. (29)

We decompose the Green tensor inside the cavity, $G(z, z', \omega) \equiv G^{(11)}(z, z', \omega)$, as given by Eq. (A1), into bulk and scattering parts G^0 and G^S , respectively,

$$G(z, z', \omega) = G^0(z, z', \omega) + G^S(z, z', \omega), \quad (\text{B1})$$

where

$$G^0(z, z', \omega) = \frac{1}{2}i \left[e^{i\beta_1(\omega)(z-z')} \Theta(z-z') + e^{-i\beta_1(\omega)(z-z')} \Theta(z'-z) \right], \quad (\text{B2})$$

and

$$G^S(z, z', \omega) = \frac{g(z, z', \omega)}{D_1(\omega)}, \quad (\text{B3})$$

with

$$g(z, z', \omega) = \frac{1}{2} \frac{e^{i\beta_1(\omega)l}}{\beta_1(\omega)} i \left[r_{13}(\omega) e^{-i\beta_1(\omega)(z-l)} \mathcal{E}^{(1)<}(z', \omega) - e^{i\beta_1(\omega)z} \mathcal{E}^{(1)>}(z', \omega) \right]. \quad (\text{B4})$$

Employing the residue theorem, we may Fourier transform $\omega^2 G^S(z, z', \omega)$ to obtain

$$\begin{aligned} f(z, z', t) &= \int \frac{d\omega}{2\pi} \omega^2 e^{-i\omega t} \frac{g(z, z', \omega)}{D_1(\omega)} \\ &= \sum_k \frac{c}{2n_1(\Omega_k)l} \Theta(t) \Omega_k^2 e^{-i\Omega_k t} g(z, z', \Omega_k). \end{aligned} \quad (\text{B5})$$

Further, the inverse transformation reads

$$\begin{aligned} \omega^2 G^S(z, z', \omega) &= \int dt e^{i\omega t} f(z, z', t) \\ &= \sum_k \frac{c}{2n_1(\Omega_k)l} \frac{i\Omega_k^2}{\omega - \Omega_k} g(z, z', \Omega_k). \end{aligned} \quad (\text{B6})$$

Then, the integration in Eq. (26) can be approximated by a principal value integration as

$$\delta\omega = -\frac{|d_{21}|^2}{\pi\hbar\epsilon_0\mathcal{A}} \mathcal{P} \int_0^\infty d\omega \frac{\omega^2}{c^2} \frac{\text{Im} G(z_A, z_A, \omega)}{\tilde{\omega}_0 - \omega}. \quad (\text{B7})$$

Using $\text{Im}G(z_A, z_A, \omega) = [G(z_A, z_A, \omega) - G^*(z_A, z_A, \omega)]/(2i)$, we insert the scattering part of the Green tensor as given by Eq. (B6) in Eq. (B7). Then, extending, in rotating-wave approximation, the integration to $\pm\infty$, we arrive, after straightforward calculation, at Eq. (29).

APPENDIX C: DERIVATION OF EQ. (31)

In the case of a high- Q cavity we are interested in, we can disregard the contribution to the integral in Eq. (28)

of the bulk part of Green function, i. e., we may let

$$\begin{aligned} G(z_A, z_A, \omega) &\mapsto G^S(z_A, z_A, \omega) \\ &= -\sum_k \frac{c^2}{\Omega_k |n_1(\Omega_k)|^2 l} \frac{1}{\omega - \Omega_k} \sin^2(\omega_k |n_1(\Omega_k)| z_A/c) \end{aligned} \quad (\text{C1})$$

in Eq. (28), where we have used Eq. (B6). In this way we obtain

$$\begin{aligned} \tilde{K}(t) &= \frac{|d_{21}|^2}{\pi\hbar\epsilon_0\mathcal{A}} \left\{ \sin^2(\omega_k |n_1(\Omega_k)| z_A/c) \right. \\ &\quad \times \int_{\Delta_k} d\omega \frac{\omega^2}{2i\omega_k |n_1(\Omega_k)|^2 l} \frac{1}{\omega - \Omega_k} e^{-i(\omega - \tilde{\omega}_0)t} \\ &\quad \left. + \sum_{k' \neq k} \sin^2(\omega_{k'} |n_1(\Omega_{k'})| z_A/c) \right. \\ &\quad \left. \times \int_{\Delta_k} d\omega \frac{\omega^2}{2i\omega_{k'} |n_1(\Omega_{k'})|^2 l} \frac{1}{\omega - \Omega_{k'}} e^{-i(\omega - \tilde{\omega}_0)t} \right\}. \end{aligned} \quad (\text{C2})$$

Since, within the approximation scheme used, the second (off-resonant) term may be regarded as being small comparing to the first one, it can be omitted. It is then not difficult to prove that, by extending the ω integration to $\pm\infty$, the first (resonant) term can be evaluated to yield Eq. (31).

APPENDIX D: DERIVATION OF EQ. (60)

Using Eqs. (A1) and (A9), we derive by straightforward calculation

$$\begin{aligned} \frac{\omega^2}{c^2} \int dz' \varepsilon''(z', \omega) G_{\text{in}}^{(3j')} (z, z', \omega) G^{(1j')*} (z_A, z', \omega) \\ = \frac{1}{2} i G^{(31)*} (z, z_A, \omega). \end{aligned} \quad (\text{D1})$$

Employing the integral relation

$$\begin{aligned} \frac{\omega^2}{c^2} \int dz' \varepsilon''(z', \omega) G(z_1, z', \omega) G^*(z_2, z', \omega) \\ = \text{Im} G(z_1, z_2, \omega) \end{aligned} \quad (\text{D2})$$

and using Eqs. (A8) and (D1), we then find that

$$\begin{aligned} \frac{\omega^2}{c^2} \int dz' \varepsilon''(z', \omega) G_{\text{out}}(z, z', \omega) G^{(1j')*} (z_A, z', \omega) \\ = -\frac{1}{2} i G^{(31)} (z, z_A, \omega). \end{aligned} \quad (\text{D3})$$

Substitution of Eq. (32) into Eq. (41) and use of Eq. (D3) eventually yield Eq. (60).

APPENDIX E: VALIDITY OF EQ. (72) INSIDE THE CAVITY

Equation (9) implies that the field (in the frequency interval Δ_k) which propagates inside the cavity from the

left to the right can be written as

$$\begin{aligned} \hat{E}_{\text{out}}^{(1)}(z, \omega) &= i\sqrt{\frac{\hbar}{\epsilon_0\pi\mathcal{A}}} \frac{\omega^2}{c^2} \\ &\times \int dz' \sqrt{\varepsilon''(z', \omega)} G_{\text{out}}(z, z', \omega) \hat{f}(z', \omega). \end{aligned} \quad (\text{E1})$$

It is straightforward to prove that the operators

$$\begin{aligned} \hat{b}_{\text{out}}^{(1)}(\omega) &= -2i\sqrt{\frac{\epsilon_0 c \pi \mathcal{A}}{\hbar \omega \Gamma_k \gamma_{\text{krad}}}} \frac{|\omega - \Omega_k|^2}{\omega - \Omega_k^*} \\ &\times t_{31}^*(\Omega_k) e^{-i\omega_k l/c} \hat{E}_{\text{out}}^{(1)}(z, \omega) \Big|_{z=0_-} \end{aligned} \quad (\text{E2})$$

($n_1 \equiv 1$) and $\hat{b}_{\text{out}}^{(1)\dagger}(\omega)$ satisfy the bosonic commutation relation

$$[\hat{b}_{\text{out}}^{(1)}(\omega), \hat{b}_{\text{out}}^{(1)\dagger}(\omega')] = \delta(\omega - \omega'). \quad (\text{E3})$$

Recalling Eq. (39), we derive

$$\hat{b}_{\text{out}}^{(1)}(\omega) |\psi(t)\rangle = F^{(1)*}(\omega, t) |1\rangle |\{0\}\rangle, \quad (\text{E4})$$

where

$$F^{(1)}(\omega, t) = \sqrt{\frac{\Gamma_k}{\gamma_{\text{krad}}}} F(\omega, t), \quad (\text{E5})$$

with $F(\omega, t)$ being given by Eq. (61). Similarly to Eq. (46), we now introduce the unitary transformation

$$\hat{b}_{\text{out } i}^{(1)}(t) = \int_0^\infty d\omega F_i^{(1)}(\omega, t) \hat{b}_{\text{out}}^{(1)}(\omega) \quad (\text{E6})$$

and make the particular choice

$$F_1^{(1)}(\omega, t) = \frac{F^{(1)}(\omega, t)}{\sqrt{\eta^{(1)}(t)}}, \quad (\text{E7})$$

where

$$\eta^{(1)}(t) \equiv \int_0^\infty d\omega |F^{(1)}(\omega, t)|^2 = \frac{\Gamma_k}{\gamma_{\text{krad}}} \eta(t). \quad (\text{E8})$$

Using Eqs. (E5) and Eq. (E8) and recalling Eq. (49), from Eq. (E7) we see that

$$F_1^{(1)}(\omega, t) = F_1(\omega, t), \quad (\text{E9})$$

which implies that the outgoing field inside the cavity can be described by the same nonmonochromatic mode functions $F_i(\omega, t)$ as the excited outgoing field outside the cavity.

Indeed, performing the calculations leading from Eq. (66) to Eq. (68) for the outgoing field inside the cavity ($-l \leq z < 0$),

$$\hat{E}_{\text{out}}^{(+)}(z) = \int_0^\infty d\omega e^{i\omega z/c} \hat{E}_{\text{out}}^{(1)}(z, \omega) \Big|_{z=0_-}, \quad (\text{E10})$$

instead of the field outside the cavity, we again arrive at an equation of the form of Eq. (68), with the same functions $\phi_i^{(1)}(z, t) = \phi_i(z, t)$, but, in general, different associated operators $\hat{b}_{\text{out } i}^{(1)}(t) \neq \hat{b}_{\text{out } i}(t)$. Only in the limit of vanishing absorption they equal each other. Performing the calculations leading from Eq. (37) to Eq. (48) for the outgoing field inside the cavity instead of the outgoing field outside the cavity, we arrive at the characteristic function

$$\begin{aligned} C_{\text{out}}^{(1)}[\beta_i(t), t] &= \exp \left[-\frac{1}{2} \sum_i |\beta_i(t)|^2 \right] \\ &\times \left[1 - \left| \sum_i \beta_i(t) \int_0^\infty d\omega F_i^{(1)}(\omega, t) F^{(1)}(\omega, t) \right|^2 \right], \end{aligned} \quad (\text{E11})$$

i.e., $F_i(\omega, t)$ and $F(\omega, t)$ in Eq. (48) are simply replaced by $F_i^{(1)}(\omega, t)$ and $F^{(1)}(\omega, t)$, respectively, where $F^{(1)}(\omega, t)$ is given by Eq. (E5), and $F_i^{(1)}(\omega, t)$ can be chosen to be $F_i(\omega, t)$.

Needless to say, that for the operator of the electric field Eq. (9) that refers to the points in the region $z < -l$, one finds

$$\hat{E}_{\text{out}}^{(0)}(z, \omega) |\psi(t)\rangle = 0. \quad (\text{E12})$$

As expected, the excited outgoing mode is restricted to the region $z \geq -l$.

APPENDIX F: DETAILS OF EQ. (94)

In Eq. (94), $\hat{B}_k(\omega, t)$ is given by

$$\begin{aligned} \hat{B}_k(\omega, t) &= \int_{\Delta_k} d\omega' \left[G_{\text{kin}}^*(\omega, \omega', t) \hat{b}_{\text{kin}}(\omega', 0) \right. \\ &\quad \left. + \sum_\lambda G_{k\lambda}^*(\omega, \omega', t) \hat{c}_{k\lambda}(\omega', 0) \right], \end{aligned} \quad (\text{F1})$$

where

$$\begin{aligned} G_{\text{kin}}(\omega, \omega', t) &= r_{31}^*(\omega) e^{i\omega' t} \delta(\omega - \omega') \\ &\quad - T_k^{*2}(\omega) v_k(\omega, \omega', t), \end{aligned} \quad (\text{F2})$$

$$G_{k\text{cav}}(\omega, \omega', t) = -T_k^*(\omega) A_{k\text{cav}}^*(\omega) v_k(\omega, \omega', t), \quad (\text{F3})$$

$$\begin{aligned} G_{k\pm}(\omega, \omega', t) &= A_{k\pm}^{(o)*}(\omega) e^{i\omega' t} \delta(\omega - \omega') \\ &\quad - T_k^*(\omega) A_{k\pm}^*(\omega) v_k(\omega, \omega', t), \end{aligned} \quad (\text{F4})$$

with

$$v(\omega, \omega', t) = \frac{1}{2\pi} \frac{c}{2n_1^*(\omega)l} \frac{e^{-i\omega\Delta t}}{\omega - \Omega_k^*} \times \left[\frac{e^{i\omega'(t+\Delta t)} - e^{i\Omega_k^*(t+\Delta t)}}{\omega' - \Omega_k^*} - \frac{e^{i\omega(t+\Delta t-t_0)} - e^{i\omega'(t+\Delta t-t_0)}}{\omega - \omega'} \right]. \quad (\text{F5})$$

In the above,

$$A_{k\pm}^{(o)}(\omega) = \frac{t_{23}(\omega)}{D_2'(\omega)} \frac{1 \pm r_{21}(\omega)e^{i\beta_2(\omega)d}}{\alpha_{\pm}(\omega)}, \quad (\text{F6})$$

$$A_{\text{cav}}(\omega) = -4i \frac{\sqrt{n_1(\omega)}}{\alpha_{\text{cav}}(\omega)}, \quad (\text{F7})$$

$$A_{\pm}(\omega) = -\frac{t_{21}(\omega)\sqrt{n_1(\omega)}}{D_2'(\omega)\alpha_{\pm}(\omega)} \times \left[r_{23}(\omega)e^{i\beta_2(\omega)d} \pm 1 \right] e^{i\beta_1(\omega)l}, \quad (\text{F8})$$

$$\alpha_{\text{cav}}(\omega) = 2\sqrt{2}|n_1(\omega)| \{n_1'(\omega) \sinh[2\beta_1''(\omega)l] - n_1''(\omega) \sin[2\beta_1'(\omega)l]\}^{-\frac{1}{2}}, \quad (\text{F9})$$

$$\alpha_{\pm}(\omega) = |n_2(\omega)|e^{i\beta_2''(\omega)d/2} \{n_2'(\omega) \sinh[\beta_2''(\omega)d] \pm n_2''(\omega) \sin[\beta_2'(\omega)d]\}^{-\frac{1}{2}}. \quad (\text{F10})$$

-
- [1] H. Walther, Phys. **54**, 617 (2006).
[2] H. Walther, B. T. H. Varcoe, B. G. Englert, and T. Becker, Rep. Prog. Phys. **69**, 1325 (2006).
[3] D. Meschede, H. Walther, and G. Müller, Phys. Rev. Lett. **54**, 551 (1985).
[4] M. Brune, J. M. Raimond, P. Goy, L. Davidovich, and S. Haroche, Phys. Rev. Lett. **59**, 1899 (1987).
[5] C. Ginzler, H.-J. Briegel, U. Martini, B.-G. Englert, and A. Schenzle, Phys. Rev. A **48**, 732 (1993).
[6] A. M. Smith and C. W. Gardiner, Phys. Rev. A **41**, 2730 (1990).
[7] G. S. Agarwal and S. Dutta Gupta, Phys. Rev. A **42**, 1737 (1990).
[8] A. D. Boozer, A. Boca, J. R. Buck, J. McKeever, and H. J. Kimble, Phys. Rev. A **70**, 023814 (2004).
[9] M. Löffler, G. M. Meyer, and H. Walther, Phys. Rev. A **55**, 3923 (1997).
[10] G. M. Meyer, M. Löffler, and H. Walther, Phys. Rev. A **56**, R1099 (1997).
[11] C. Di Fidio, W. Vogel, R. L. de Matos Filho, and L. Davidovich, Phys. Rev. A **65**, 013811 (2001).
[12] R. L. de Matos Filho, J. C. Retamal, and N. Zagury, Phys. Rev. A **73**, 013808 (2006).
[13] C. Monroe, Nature **416**, 238 (2002).
[14] C. H. Bennett and P. W. Shor, IEEE Trans. Inf. Theory **44**, 2724 (1998).
[15] N. Lütkenhaus, Phys. Rev. A **61**, 52304 (2000).
[16] J. I. Cirac, P. Zoller, H. J. Kimble, and H. Mabuchi, Phys. Rev. Lett. **78**, 3221 (1997).
[17] E. Knill, R. Laflamme, and G. J. Milburn, Nature **409**, 461 (2001).
[18] A. S. Parkins, P. Marte, P. Zoller, and H. J. Kimble, Phys. Rev. Lett. **71**, 3095 (1993).
[19] J. McKeever, A. Boca, A. D. Boozer, R. Miller, J. R. Buck, A. Kuzmich, and H. J. Kimble, Science **303**, 1992 (2004).
[20] M. Hennrich, T. Legero, A. Kuhn, and G. Rempe, Phys. Rev. Lett. **85**, 4872 (2000).
[21] T. Wilk, S. C. Webster, H. P. Specht, G. Rempe, and A. Kuhn, Phys. Rev. Lett. **98**, 063601 (2007).
[22] A. Kuhn, M. Hennrich, and G. Rempe, Phys. Rev. Lett. **89**, 067901 (2002).
[23] M. Keller, B. Lange, K. Hayasaka, W. Lange, and H. Walther, Nature **431**, 1075 (2004).
[24] E. T. Jaynes and F. W. Cummings, Proc. IEEE **51**, 89 (1963).
[25] M. J. Collett and C. W. Gardiner, Phys. Rev. A **30**, 1386 (1984).
[26] C. W. Gardiner and M. J. Collett, Phys. Rev. A **31**, 3761 (1985).
[27] G. W. Gardiner and P. Zoller, *Quantum Noise* (Springer, Berlin, 2001), 3rd ed.
[28] M. Khanbekyan, L. Knöll, A. A. Semenov, W. Vogel, and D.-G. Welsch, Phys. Rev. A **69**, 043807 (2004).
[29] F. Haake, *Statistical Treatment of Open System by Generalized Master Equations* (Springer, Berlin, 1973), vol. 66 of *Springer Tracts in Modern Physics*.
[30] W. H. Louisell, *Quantum Statistical Properties of Radiation* (Wiley, New York, 1973).
[31] E. B. Davies, *Quantum Theory of Open Systems* (Academic Press, New York, 1976).
[32] J. Dalibard, Y. Castin, and K. Mølmer, Phys. Rev. Lett. **68**, 580 (1992).
[33] R. Dum, A. S. Parkins, P. Zoller, and C. W. Gardiner, Phys. Rev. A **46**, 4382 (1992).
[34] H. J. Carmichael, *An Open System Approach to Quantum Optics* (Springer, Berlin, 1993), vol. m18 of *Lecture Notes in Physics, New Series m: Monographs*.
[35] L. Knöll, S. Scheel, and D.-G. Welsch, *Coherence and Statistics of Photons and Atoms* (Wiley, New York,

- 2001), chap. 1, quant-ph/0003121.
- [36] W. Vogel and D.-G. Welsch, *Quantum Optics* (Wiley-VCH, Weinheim, 2006), third, revised and extended ed.
- [37] L. Knöll, W. Vogel, and D.-G. Welsch, *Phys. Rev. A* **43**, 543 (1991).
- [38] R. W. F. van der Plank and L. G. Suttrop, *Phys. Rev. A* **53**, 1791 (1996).
- [39] C. Viviescas and G. Hackenbroich, *Phys. Rev. A* **67**, 013805 (2003).
- [40] C. Viviescas and G. Hackenbroich, *Journal of Optics B: Quantum and Semiclassical Optics* **6**, 211 (2004).
- [41] H. Feshbach, *Ann. Phys.* **19**, 287 (1962).
- [42] S. M. Dutra and G. Nienhuis, *Phys. Rev. A* **62**, 063805 (2000).
- [43] M. Khanbekyan, L. Knöll, D.-G. Welsch, A. A. Semenov, and W. Vogel, *Phys. Rev. A* **72**, 053813 (2005).
- [44] A. A. Semenov, D. Y. Vasylyev, W. Vogel, M. Khanbekyan, and D.-G. Welsch, *Phys. Rev. A* **74**, 033803 (2006).
- [45] A. A. Semenov, W. Vogel, M. Khanbekyan, and D.-G. Welsch, *Phys. Rev. A* **75**, 013807 (2007).
- [46] M. Ley and R. Loudon, *J. Mod. Opt.* **34**, 227 (1987).
- [47] D. Meiser and P. Meystre, *Phys. Rev. A* **74**, 065801 (2006).
- [48] M. S. Tomas, *Phys. Rev. A* **66**, 052103 (2002).
- [49] Note that in the multipolar-coupling scheme, $\hat{\mathbf{E}}(\mathbf{r})$ may behave like a displacement field with respect to the atomic polarization field.